J Mol Model (2005) 11: 489–502
DOI 10.1007/s00894-005-0258-5

ORIGINAL PAPER

**Mathias-Costa Blaise · Ramanathan Sowdhamini**
**Nithyananda Pradhan**

# Comparative analysis of different competitive antagonists interaction with NR2A and NR2B subunits of *N*-methyl-D-aspartate (NMDA) ionotropic glutamate receptor

Received: 4 October 2004 / Accepted: 22 February 2005 / Published online: 1 June 2005


**Abstract** The antagonist-bound conformation of the NR2A and NR2B subunits of *N*-methyl-D-aspartate (NMDA) ionotropic glutamate receptor are modeled using the crystal structure of the DCKA (5,7-dichlorokynurenic acid)-bound form of the NR1 subunit ligand-binding core (S1S2). Five different competitive NMDA receptor antagonists [(1) DL-AP5; (2) DL-AP7; (3) CGP-37847; (4) CGP 39551; (5) (RS)-CPP] have been docked into both NR2A and NR2B subunits. Experimental studies report NR2A and NR2B subunits having dissimilar interactions and affinities towards the antagonists. However, the molecular mechanism of this difference remains unexplored. The distinctive features in the antagonist's interaction with these two different but closely related (~80% sequence identity at this region) subunits are analyzed from the patterns of their hydrogen bonding. The regions directly involved in the antagonist binding have been classified into seven different interaction sites. Two conserved hydrophilic pockets located at both the S1 and S2 domains are found to be crucial for antagonist binding. The positively charged (*Lys*) residues present at the second interaction site and the invariant residue (*Arg*) located at the fourth interaction site are seen to influence ligand binding. The geometry of the binding pockets of NR2A and NR2B subunits have been determined from the distance between the C-α atoms in the residues interacting with the ligands. The binding pockets are found to be different for NR2A and NR2B. There are gross dissimilarities in competitive antagonist binding between these two subunits. The binding pocket geometry identified in this study may have the potential for future development of selective antagonists for the NR2A or NR2B subunit.

**Keywords** NMDA receptor · Homology modeling · Docking · NR2A · NR2B · Competitive antagonist · Binding pocket

M.-C. Blaise · N. Pradhan (✉)
Department of Psychopharmacology,
National Institute of Mental Health
and Neuro Sciences (NIMHANS),
Bangalore, 560029, India
E-mail: npr@nimhans.kar.nic.in
Tel.: +91-80-6995108
Fax: +91-80-6564830

R. Sowdhamini
National Centre for Biological Sciences (NCBS),
TIFR, UAS-GKVK Campus, Bangalore, 560065, India

## Introduction

The NMDA subtype of the glutamate receptor belongs to a subfamily of ionotropic receptors with distinctive functional and biophysical properties. The NMDA receptors are involved in synaptic plasticity, learning and memory, brain development and excitotoxicity [1–3]. Molecular cloning has identified a family of genes that code for subunits of ionotropic glutamate receptors [4, 5], Glutamate receptor 1–4 codes for the AMPA type of glutamate receptor. Five other genes (NR1 and NR2A-2D) code for NMDA receptor subunits. The NR1 subunit is widely distributed throughout the mammalian brain, whereas the NR2 subunits are differentially expressed in distinct brain regions in an age-dependent manner [6–8]. It is postulated that the functional NMDA receptors are hetero-tetramers composed of two NR1 and two NR2 subunits [9]. This receptor activation requires simultaneous occupation of two independent glycine and glutamate binding sites located on the NR1 and NR2 subunits, respectively [10–14].

The NMDA receptor is the major therapeutic target for a wide range of cerebral dysfunctions such as stroke, analgesia, epilepsy and many neurodegenerative disorders [15]. Therapeutic implications warrant a clear understanding of the heterogeneity of NMDA receptors for the development of subtype-specific compounds [15–17]. Currently, several glycine site (NR1) competitive antagonists are in various stages of development [18]. Unfortunately, the NR1 subunit forms an essential component to all functional NMDA receptors [9].

Therefore, certain disadvantages are associated with the glycine site antagonism, where these drugs may act on all the NMDA receptors without selectivity. In contrast, all the NR2 subunits (glutamate binding site) are not mandatory for functional NMDA receptors. Further, NR2 is expressed in a distinct spatiotemporal manner [7, 8] making it a suitable alternative target for competitive antagonism [19–23].

The ligand-binding sites in all the ionotropic glutamate receptors (iGluRs) are formed by two domains; S1, located at the N terminal and S2 in the M3–M4 linker [24]. The ligand-binding core of NR1 and iGluR2 has been crystallized recently in agonist and antagonist-bound forms [25, 26]. The S1-S2 structure reveals two lobes connected by a hinge forming a clamshell-like structure similar to the bacterial periplasmic binding protein [27]. The crystallographic data of NR1 and AMPA indicate the feasibility of modeling S1S2 domain, wherein the S1S2 domains remain closed upon agonist binding and interaction with an antagonist opens the S1S2 construct towards the unbound (open-apo) state [25, 26]. Studies have shown conformational changes of the S1S2 domain in characterizing the iGluR agonist and antagonist activity by calculating the degree of S1S2 domain closing and opening, respectively [28]. The opening and closing of the S1S2 domain conformation is found to correlate with ion-channel properties [24, 26, 28]. The availability of several ligand-binding core crystal templates have generated recent interest in the binding core of different NMDA receptor subunits [13, 29–32]. Nevertheless, templates with more identity in query sequences belonging to the same subfamily are expected to produce better models than those obtained earlier by using low sequence-similarity templates [33]. Among the NR2 subunits, NR2A and NR2B are of functional significance [3, 34]. Although NR2A and NR2B subunits share ~80% sequence identity in the ligand-binding region, not all the NR2 subunit-specific competitive antagonists bind with these subunits in the same mode and affinity [35, 36].

The NR2A and NR2B subunits have similar pharmacological profiles for glutamate binding while there are significant differences in their relative affinity towards agonists and antagonists [37]. Compared to the NR2B subunit, NR2A has a higher affinity towards antagonists and a lower affinity towards agonists [19, 37–40]. This functional distinction remains unclear. Therefore, Tikhonova et al. [30] suggest that it may hardly be possible to design subtype-selective antagonists for the glutamate binding site of the NMDA receptor. This is attributed to the distance between the ligand and the nearest non-conserved amino acids among the NR2A-2D subtype exceeding 7.5 Å, and also due to the lack of free space between them. Our analysis provides a three-dimensional comparative view of the antagonist binding core of the NR2A and NR2B subunits. The results may be of use for future development of subunit specific NMDA receptor antagonists.

## Materials and methods

### Model building

The primary sequences of the NR2A and NR2B subunits were obtained from the NCBI database and analyzed by using the BLASTP [41] program. Secondary structure prediction was carried out by PHDsec [42] and CLUSTAL X [43] was used for multiple sequence alignment. The X-ray crystal structure of NR1 (1pbq) was used as a template to model the antagonist-bound conformation of the NR2A and NR2B ligand-binding cores. The multiple sequence alignment of the NR2A and NR2B subunits with NR1 has been carried out with 40 iGluR sequences. All the aligned sequences are available as Electronic Supplementary Material-1 (ESM-1) (http://link.springer.de) along with J Mol Model 2004 (5–6):305–316. Twenty models are prepared for each subunit using MODELLER (spatial restraint method) [44] and ranked by the analysis of their 3D profile by Verify3D [45] and stereochemistry using PROCHECK [46]. From these observations, the highest ranking model was selected and subjected to energy minimization using the AMBER force field as available in the InsightII [47] molecular modeling software (Accelrys Inc., USA). All energy minimizations in this study were carried out with a minimum of 1000 iterations by the steepest descendent and conjugate gradient methods. The N and C terminals of the models were not charged during minimization. Hydrogen atoms were added to the protein models to facilitate incorporating hydrogen bonds.

### Docking

All the antagonists (Fig. 1) were designed by using the InsightII/Builder module. The 3D models of the antagonists were optimized using the facility provided in the same module. Information available from known crystal structures and mutagenesis data [25, 26, 12] were used to determine the putative ligand-binding pocket of the NR2A and NR2B models. Each antagonist was placed at the binding region and the ligand–receptor complex was subjected to energy minimization. An automated docking method (fixed-docking) available in INSIGHTII was used to dock all the antagonists used in this study. In order to rearrange the conformation of the ligand–receptor complex, after each docking a short molecular dynamics simulation was performed for 10 pS using the discover 3 module of InsightII. The docking experiment generates several orientations of the drug towards of the receptor. The final orientation of the drug towards the receptor is obtained by reminimization of the drug–receptor complexes. LSQMAN [48] was used to superimpose the models onto their templates and to calculate the rmsd of different models. The 4 Å radius spheres are created around the antagonists to identify

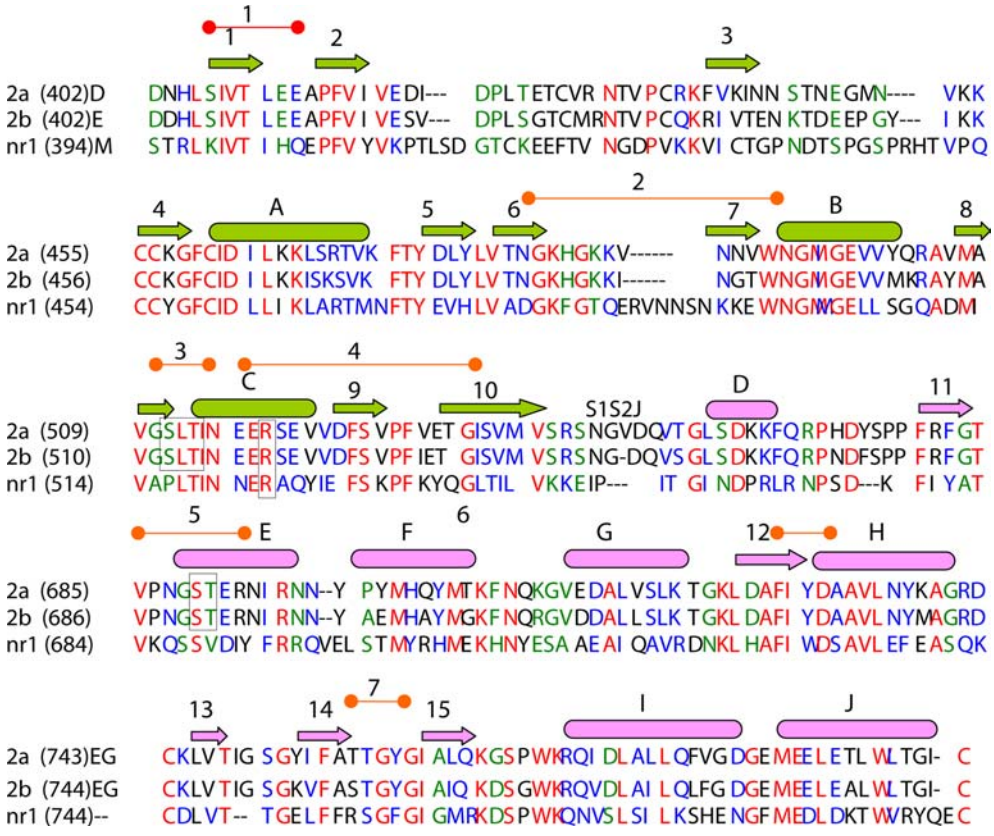


**Fig. 1** The multiple sequence alignment of NR2A and NR2B subunits with the ligand-binding core of NR1 (*template*) are depicted with α-helices (*cylinder shape*) and α-strands (*arrow head*) colored in green and pink at the S1 and S2 segments, respectively, and numbered accordingly. The junction between the S1 and S2 segments is marked as S1S2J. Drug–receptor interaction sites are marked by the "**o**——**o**" symbol and numbered from one to seven. The residues located at the interface of the S1S2 domain in all the drug bound conformations are shown in *box*

the residues involved in both bonded and non-bonded interactions. The drug–receptor binding scores were studied using the LUDI scoring method [49, 50]. The NCBI database numbering is used to identify the amino acids throughout the study. All the modeling figures were prepared using the INSIGHTII software.

## Results

### Modeling the antagonist bound conformation of NR2A and NR2B ligand-binding core

Sequence analysis, alignment (Fig. 2), and homology modeling were carried out by the methods described above [51]. The models revealed ten well conserved α-helices and 15β-strands in the S1S2 domain. The S2 domain contained more long α-helices than the S1 domain whereas β-strands are more frequent in the S1 than in the S2 domain. Four sets of β-sheets were found in the models, among which three were anti-parallel and one was parallel. The three anti-parallel β-sheets are formed by 3–4β, 8–15β and 10–14β pairs of β-strands. The parallel sheet is formed by 1–5β strands. The anti-parallel 8–14β sheet located at the S1 domain was directly involved in ligand binding. The tip of parallel 1–5β-sheet oriented the ligand positions, facilitating its interaction with S2 domain residues. The anti-parallel 10–13β-sheet located at the interface of the S1S2 domain is not involved in ligand binding directly. It is not in the vicinity of the ligand-binding regions. The conserved *Cys* residues located next to *H* and *J-α-helix* of both NR2A (*Cys745* and *Cys800*) and NR2B (*Cys746* and *Cys801*) subunits are found to make a disulphide bond influencing the movements in the S1S2 domain. The region involved in ligand binding is divided into seven interaction sites (marked red in Fig. 1) to explain the location of interactive residues conveniently (Table 1).

### Drug-A: [DL-AP5 (DL-2-amino-5-phosphonopentanoicacid)]

*Known as: AP-5*

Partially automated docking, energy minimization and small molecular dynamics simulation (10 ps) reveal a projection of the $PO(OH)_2$ group of *AP5* towards *Thr514* and *Glu413* of the S1 domain in NR2B. The α-carboxylic group of AP5 is found to interact with *Thr691 (*at *Eα-helix*) and its amino group interacts with the electron rich aromatic amino acid *Tyr762* and charged *Asp763* (seventh interaction site) of the S2 domain (Fig. 3a, b). The hydrophilic environment created by the highly conserved *Ser512*, *Thr514* residues interacts with the ligand in the NR2A and NR2B subunits of the NMDA receptor. In NR2A, the $PO(OH)_2$ group of *AP5* interacts with *His485* (Fig. 3a) and the α-amino and carboxylic group penetrated into the S2 domain making interactions with *Asn693* and *Thr759*.

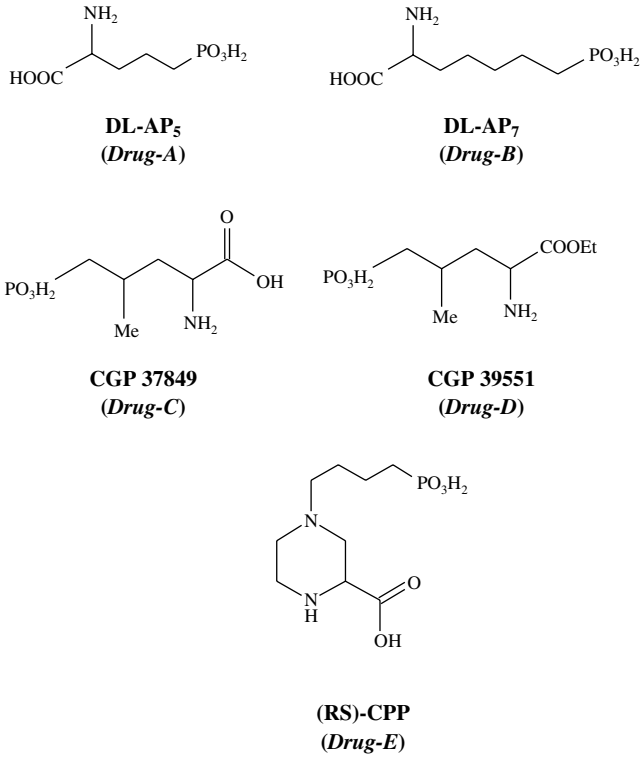


**Fig. 2** Selective NMDA receptor (*competitive*) antagonists used in this study shown here are: DL-AP5, DL-2-amino-5-phosphonopentanoic acid (*Drug-A*), DL-AP7, DL-2-amino-7-phosphonoheptanoic acid (*Drug-B*), CGP 37849, (E)-(±)-2-amino-4-methyl-5-phosphono-3-pentanoic acid (*Drug-C*), CGP 39551, (E)-(±)-2-amino-4-methyl-5-phosphono-3-pentanoic acid ethyl ester (*Drug-D*) and (RS)-CPP, (RS)-3-(2-Carboxypiperazin-4-yl) propyl-1-phosphonic acid (*Drug-D*)

Although similar kinds of interactions are observed for NR2B, the AP5-binding mode is different. The *Arg518* interaction in NR2A is conspicuously absent in NR2B with the equivalent residue *Arg519*. The number of hydrogen bonds between ligand and receptor are different for the NR2A and NR2B subunits (Table 2). The agonists kept the S1S2 domain in a closed state, whereas the antagonists kept the S1S2 domain in its detached state. The rmsd difference between the antagonist and the agonist-bound conformations of the NR2B–AP5 complex (∼2 Å) is more than for the NR2A–AP5 complex (∼1.6 Å) but this difference might be insignificant. It merely points to the proportionality of domain detachment with antagonist activity. The presence of phosphonic acid and carboxylic acid groups at the either end of *AP5* and other drugs may be crucial for domain detachment.

## Drug-B: [DL -AP (DL-2-amino-7-phosphonoheptanic acid)]

*Known as: AP-7*

Increasing the distance between the phosphonic acid and α-amino group by the addition of an ethyl group in *AP5* resulted in enhanced antagonist activity in AP7 [52]. The mode of binding of *AP7* is different from that of AP5 in respect to the NR2A and NR2B subunits. *AP7* does not bind in the expected configuration like a wedge between the S1S2 domains (Fig. 4a, b). The *AP7* molecule makes a complex at the hydrophilic cavity created by the side chain of *Ser* and *Thr* residues of S1S2 domains in NR2A and NR2B. Unlike other drugs, *AP7* possesses a strong interaction with the first, second and third interaction sites of the S1 domain shown in Table 1. Similar interaction is not observed in NR2A. AP7 is found to interact at the sixth and seventh interaction sites of NR2A but not with NR2B. In the S1 domain of NR2A, *Ser511* and *Thr513* located in between *8th*β and *C*-α *helix* are separated by a *Leu* residue, whereas it is continuous at S2 (*Ser689* and *Thr690 at E*-α-*helix*) domain to accommodate the α-amino and α-carboxylic acid groups of both AP5 and AP7.

*Arg518* and *Arg519* are found to be the key residues interacting with *AP7* in NR2A and NR2B, respectively. In the case of other antagonists at least one of these two subunits fails to have the *Arg* interaction (Table 1 and Fig. 4a, b). The conformation of the amino group of the AP7 is opposite in direction for the NR2A and NR2B subunits, which results in it having no hydrogen bonding with the OH group of *Ser689* of the NR2A subunit while it makes a H-bond with *Ser689* in NR2B. NR2A had two hydrogen-bonded interactions with the drug, whereas NR2B (Lys488) makes only one such interaction with the fourth oxygen atom of AP7 (Table 2). The distance between the $PO(OH)_2$ and the amino-acid group in AP7 is 7.3 Å in NR2B, whereas it is only 6.8 Å in NR2A after docking. Thus, rotation about the bonds (torsion) of AP7 differed between the NR2A and NR2B subunits, which may reflect the difference in ligand–receptor interactions.

## Drug-C: 2-amino-4-methyl-5-phosphono-3-pentenoic acid

*Known as: CGP 37849*

The NR2A has several non-bonded interactions with S2 domain residues at the first, fifth and sixth interaction sites with CGP 37849 (*drug-c*). Similar interactions are very few or not observed at the same (interaction sites 1 and 6) regions of the NR2B ligand-binding core (Fig. 5a, b). Conformations of the drug molecules in the two subunits are similar and a lower number of bonded interactions was identified in antagonist docking. Comparatively, *drug-c* interacts with more amino acids in the NR2A subunit than the other drugs. In the NR2B subunit, the amino acids are packed around the drug. The binding-pocket residues are rather dispersed in NR2A. The *Arg519* residue of the NR2B subunit is involved in a non-bonded interaction with *drug-c*, whereas the equivalent residue

**Table 1** Interaction of selective NMDA receptor (competitive) antagonists with NR2A and NR2B subunits

| No. of i interaction sites | Interaction sites | AP5 (Drug-A) | | AP7 (Drug-B) | | CGP 37849 (Drug-C) | | CGP 39551 (Drug-D) | | (RS)-CPP (Drug-E) | |
|---|---|---|---|---|---|---|---|---|---|---|---|
| | | NR2A | NR2B | NR2A | NR2B | NR2A | NR2B | NR2A | NR2B | NR2A | NR2B |
| S1 Domain | | | | | | | | | | | |
| 1 | Loop b/w1β and 2β | Leu411 Glu413 His485 | Glu413 | Glu413 Phe416 | Leu411 Glu412 Glu413 | Leu411 Glu413 Phe416 | – | Leu411 Glu413 Pro415 Phe416 | **Glu413** | Glu413 | **Glu413** |
| 2 | Loop b/w 6 β and 7 β | His485 | – | Lys484 His485 | His486 **Lys488** Lys489 Tpr494 Met497 | Gly483 Lys484 His485 | His486 Gly487 Lys488 Lys489 | His485 | His486 **Gly487** Lys488 Lys489 Tpr494 | Lys484 His485 Gly486 Lys487 | His486 Lys488 |
| 3 | Loop b/w 8β and C-α | Ser511 Leu512 Thr513 | Thr514 | Ser511 Leu512 **Thr513** | Ser512 Leu513 Thr514 | Ser511 Thr513 | **Ser512** Leu513 Thr514 Asn516 | **Ser511** Thr513 | Ser512 Leu513 Thr514 | Ser511 Thr513 | Ser512 |
| 4 | Region b/w C-α and 10β | **Arg518** | **Thr532** Gly533 Ile534 | Arg518 | Asn518 Arg519 | Thr531 | Arg519 | **Arg518** | Arg519 | Arg518 Gly532 Ile533 | – |
| S2 Domain | | | | | | | | | | | |
| 5 | Helix E-α | **Ser689** | Ser690 **Thr691** | - | Ser690 | Val685 Gly688 Ser689 Thr690 | Ser690 | Ser689 **Arg692** | **Ser690** | Gly688 Ser689 | Asn688 Gly689 Ser690 **Thr691** |
| 6 | Region b/w 12β andH-α | Tyr730 Asp731 | Tyr731 Asp732 Ala733 | Tyr730 **Asp731** Ala733 | Tyr731 | Tyr730 Asp731 Val734 | – | Tyr730 Asp731 Ala733 Val734 | Tyr731 **Asp735** Val735 | Tyr730 Asp731 | Tyr731 Asn732 Val735 |
| 7 | B/w 14β and 15β | Tyr761 | Ala758 Thr760 Tyr762 | Tyr761 | – | Tyr761 | Tyr762 | Tyr761 | Tyr762 | Tyr761 | – |

The seven interaction sites have been numbered and described in *columns 1 and 2*, respectively. The residues involved in hydrogen bonding with the drug are shown in *bold*

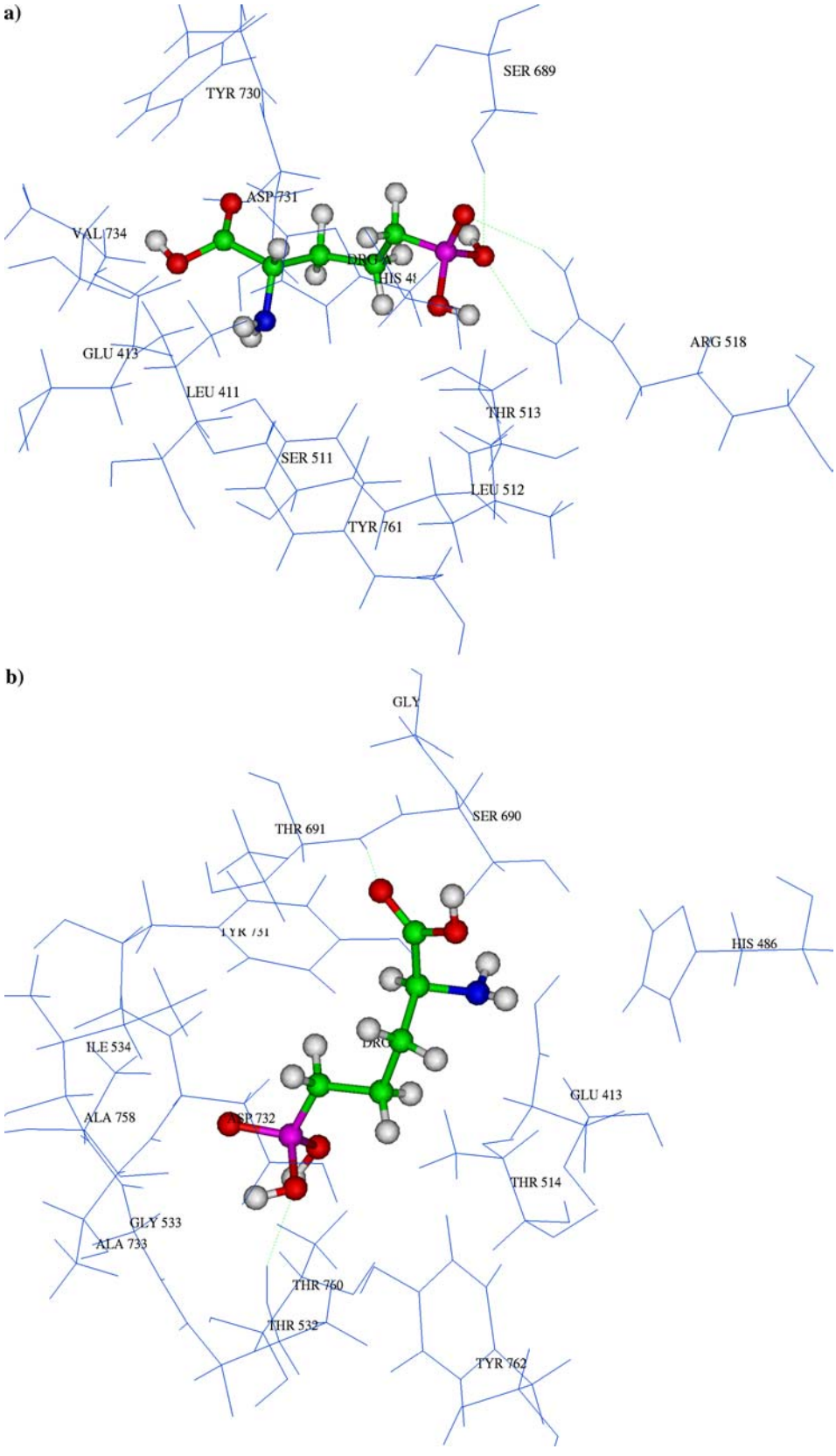


**Fig. 3** **a** shows the interactions of Drug A with the NR2A subunit of the NMDA receptor. **b** show the interactions of Drug A with NR2B subunit of the NMDA receptor. The amino acids shown here are within 4 Å radius of drug. Hydrogen bonds between the drug and receptor are marked in *green dotted lines*. Drugs are rendered in cpk (*ball* and *stick*) and amino acids are shown in *blue color* (*lines*)

(*Arg518*) in NR2A subunit has no interaction. NR2A possesses a strong interaction with several *E-α-helix* residues, whereas the NR2B interaction is limited to the *Ser690* residue of the helix. Only one hydrogen bond is observed in both the subunits but dissimilar residues are found to interact with the drug.

**Table 2** The hydrogen-bonding pattern between the antagonists and NR2A/NR2B subunits

| Sl No. | Name of the Subunit | Donor | Acceptor | Distance | Angle |
|---|---|---|---|---|---|
| DL-AP5 (Drug-A) | NR2A | Arg518:HH21 | Drg:O3 | 2.27 | 136.77 |
| | | Arg105:HH11 | Drg:O5 | 2.44 | 146.17 |
| | | Ser689:HG | Drg:O5 | 2.20 | 157.08 |
| | NR2B | Thr532:HG1 | Drg:O5 | 1.98 | 155.83 |
| | | Thr691:HN | Drg:O2 | 2.19 | 166.96 |
| DL-AP7 (Drug-B) | NR2A | Ap7:H5 | Asp197:OD1 | 2.17 | 148.66 |
| | | Ap7:H3 | Thr513:OG1 | 2.25 | 122.29 |
| | NR2B | Lys488:HN | Drg:O4 | 2.39 | 131.29 |
| CGP-37847 (Drug-C) | NR2A | His485:ND1 | Drg:O4 | 2.70 | * |
| | NR2B | Drg:HN2 | Ser512:O | 2.46 | 140.24 |
| CGP 39551 (Drug-D) | NR2A | Drg:HN2 | Ser511:O | 2.32 | 140.31 |
| | | Arg105:HH21 | Drg:O5 | 1.77 | 170.55 |
| | | Arg692:HH11 | Drg:O3 | 1.73 | 143.35 |
| | | Arg692:HH21 | Drg:O5 | 1.78 | 135.85 |
| | NR2B | Glu413:HE2 | Drg:O4 | 2.20 | 158.86 |
| | | Drg:HO | Gly487:O | 2.02 | 146.78 |
| | | Ser690:HG | Drg:O | 2.00 | 152.22 |
| | | Tyr731:HH | Drg:O3 | 2.03 | 156.57 |
| | | Asp732:HD2 | Drg:O3 | 1.68 | 153.10 |
| (RS)-CPP (Drug-E) | NR2A | – | – | – | – |
| | NR2B | Drg:H5 | Gln413:OE2 | 2.45 | 136.73 |
| | | Gln413:HE2 | Drg:O5 | 2.35 | 150.77 |
| | | Thr691:HN | Drg:O3 | 2.24 | 140.50 |

*Not applicable. The atom numberings in *columns 3 and 4* are according to the INSIGHT-II software

Drug-D: 2-amino-4-methyl-5-phosphono-3-pentanoic acid ethyl ester

*Known as: CGP 39551*

The mode of binding of CGP 39551 (*drug-d*) is entirely different for NR2A and NR2B. In the NR2B subunit, the phosphonoic acid group of *drug-d* is involved in bonded interactions with *Arg519*, but a similar interaction is absent for the NR2A subunit (Fig. 6a, b). The ethyl ester group of the drug molecule interacts with the second interaction site and with the *Trp494* residue in NR2B, whereas it had weak interactions in the NR2A subunit (restricted to *His485* residue only). The methyl group of *drug-d* interacts with a conserved *Ser* residue in both the NR2A and 2B subunits. The methyl group interaction in *drug-d* is similar to that observed with *drug-c*. The conformations of the drug molecule do not show significant differences for the NR2A and NR2B subunits. Selectively, the first and third interaction sites of S1 domain contributed drug-*d* binding in NR2A whereas all other sites in both NR2A and NR2B are involved in drug interaction (Table 1). In most of the hydrogen bonds, the electron acceptors are the electronegative oxygen atoms located at both the ends of the *drug-d* molecule (Table 2).

Drug-E: (RS)-3-(2-carboxpiperzine-4-yl)-propyl-1-phosphonic acid

*Known as: (RS)-CPP*

The carboxyl group attached to the piperazin ring of *drug-e* interacts with the residues located at the second interaction site and the NH group of the piperazin ring interacts with the guanidium group of *Arg518* of NR2A. However, similar interactions are not observed in NR2B (Fig. 7a, b). The fifth and sixth interaction sites contributed to *drug-e* binding to the NR2B subunit. The hydroxyl group present at the phosphonic acid group of drug-e interacted with the OH group of *Ser689* and with the methyl group of the *Ile533* side chain of NR2B. The presence of electron rich phosphonic acid and carboxylic acid groups at either end of the drug enhance bonded and non-bonded interactions with the residues in both the subunits of NMDA receptor. The plane of the piperazin ring of the drug is oriented perpendicular to the axis of the propyl chain and the phophonoic acid in both NR2A and 2B subunits. The conformation of the ligand in the binding pocket differs for these subunits. *Drug-e* seems to produce a different mode of interaction with NR2A and NR2B subunits by having three hydrogen bonds with the NR2B subunit but none with NR2A.

*Geometry of the ligand-bonding pockets*

We have calculated the geometry of ligand-binding pocket from appropriate ligand–receptor complexes of the five drugs with NR2A and NR2B subunits. The distance between $c_\alpha$ atoms of the six crucial residues forming the binding pocket are measured in all the sets of drug–receptor complexes. The geometry of the ligand-binding pocket reveals significant differences in the distance and angle between the crucial residues of NR2A and NR2B (Table 3).

*Drug–receptor binding score*

The drug–receptor-binding scores (Table 4) indicate *drug-D* binds more effectively in both NR2A and NR2B

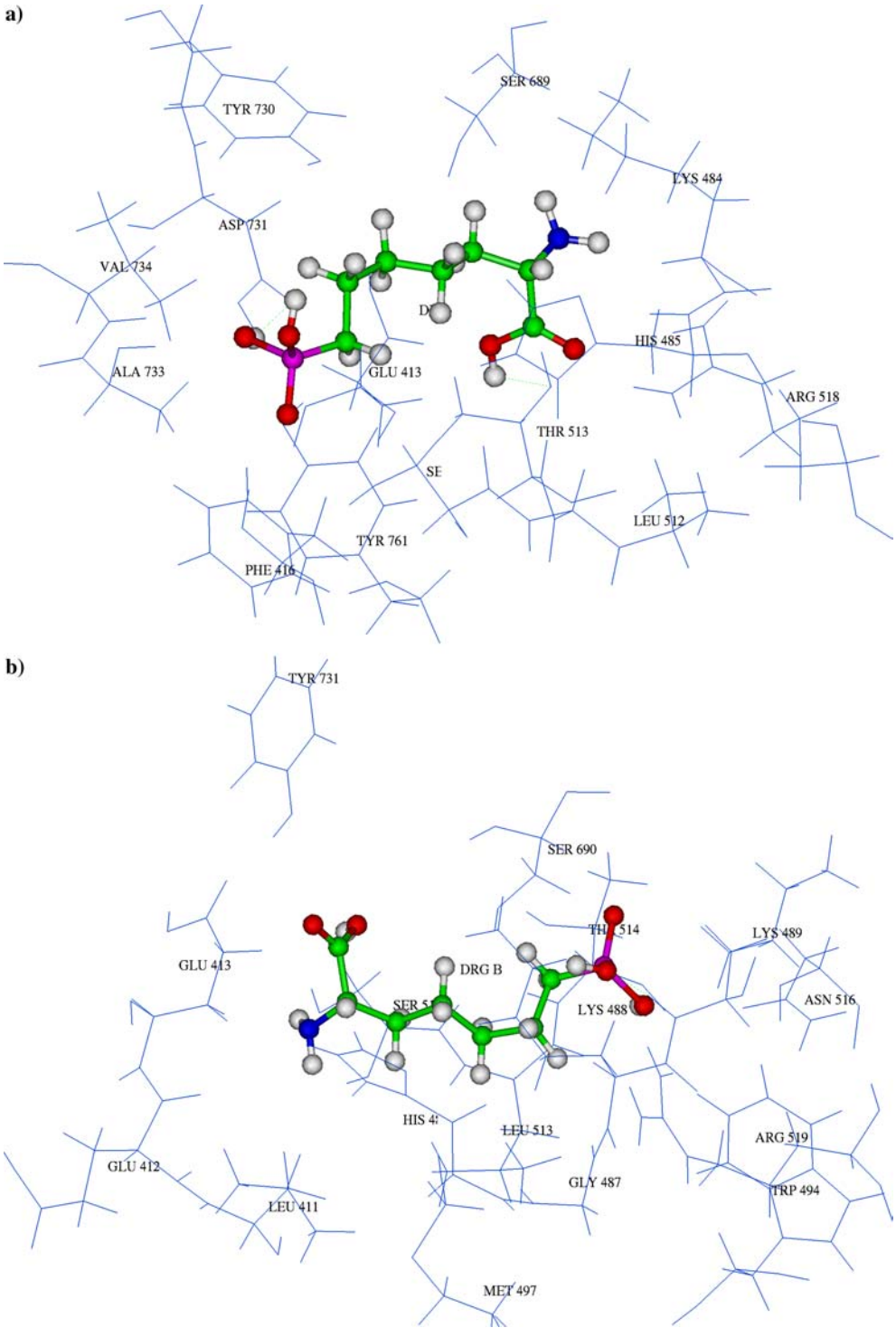


**Fig. 4** **a** shows the interactions of Drug-B with the NR2A subunit of the NMDA receptor. **b** show the interactions of Drug-B with NR2B subunit of the NMDA receptor. The amino acids shown here are within 4 Å radius of drug. Hydrogen bonds between the drug and receptor are marked in *green dotted lines*. Drugs are rendered in cpk (*ball* and *stick*) and amino acids are shown in *blue color* (*lines*)

subunits than any other drug. Further, its binding score with the NR2B subunit is significantly higher than the NR2A. This increase in binding score is due to the higher number of hydrogen bonded interactions as well as higher aliphatic/aromatic lipophilic (hydrophobic) interactions in *drug-D*. Except for the *drug-E*, the percentages of surface in contact with the receptor do not differ significantly for the drugs analyzed here. The $\Delta G_{rot}$ term indicates that the number of degrees of freedom of *drug-B* is higher than for any other drugs. *Drug-A*, *B* and *C* show almost similar scores in several parameters of the LUDI analysis. Consequently, *drug-A*, *B* and *C* are found to be equally poor in their binding properties with the receptor. Nevertheless, the result of *drug-E is* comparable with *drug-D* in terms the lipophilic interactions.

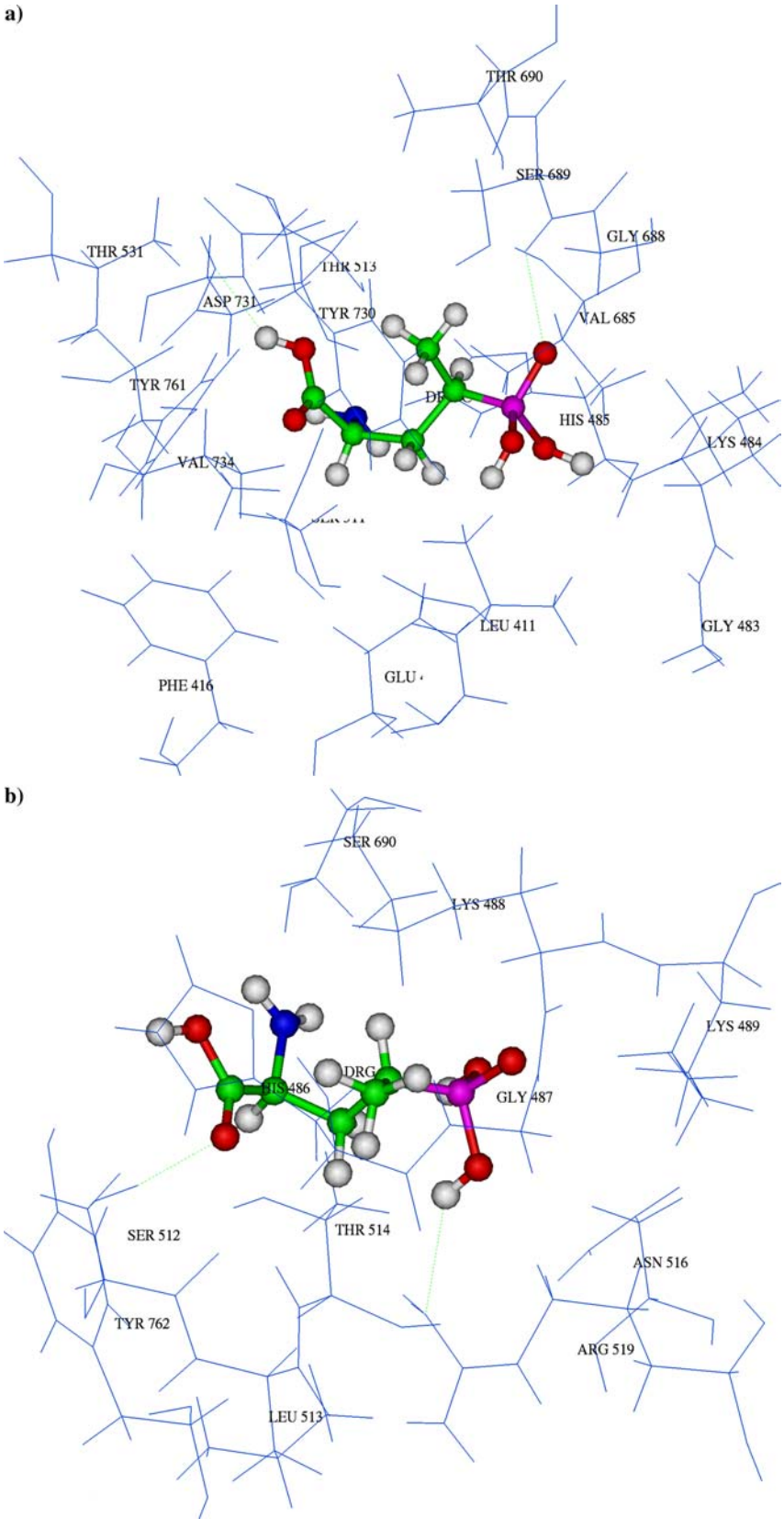


**Fig. 5** **a** shows the interactions of Drug-C with the NR2A subunit of the NMDA receptor. **b** show the interactions of Drug-C with NR2B subunit of the NMDA receptor. The amino acids shown here are within 4 Å radius of drug. Hydrogen bonds between the drug and receptor are marked in *green dotted lines*. Drugs are rendered in cpk (*ball* and *stick*) and amino acids are shown in *blue color* (*lines*)

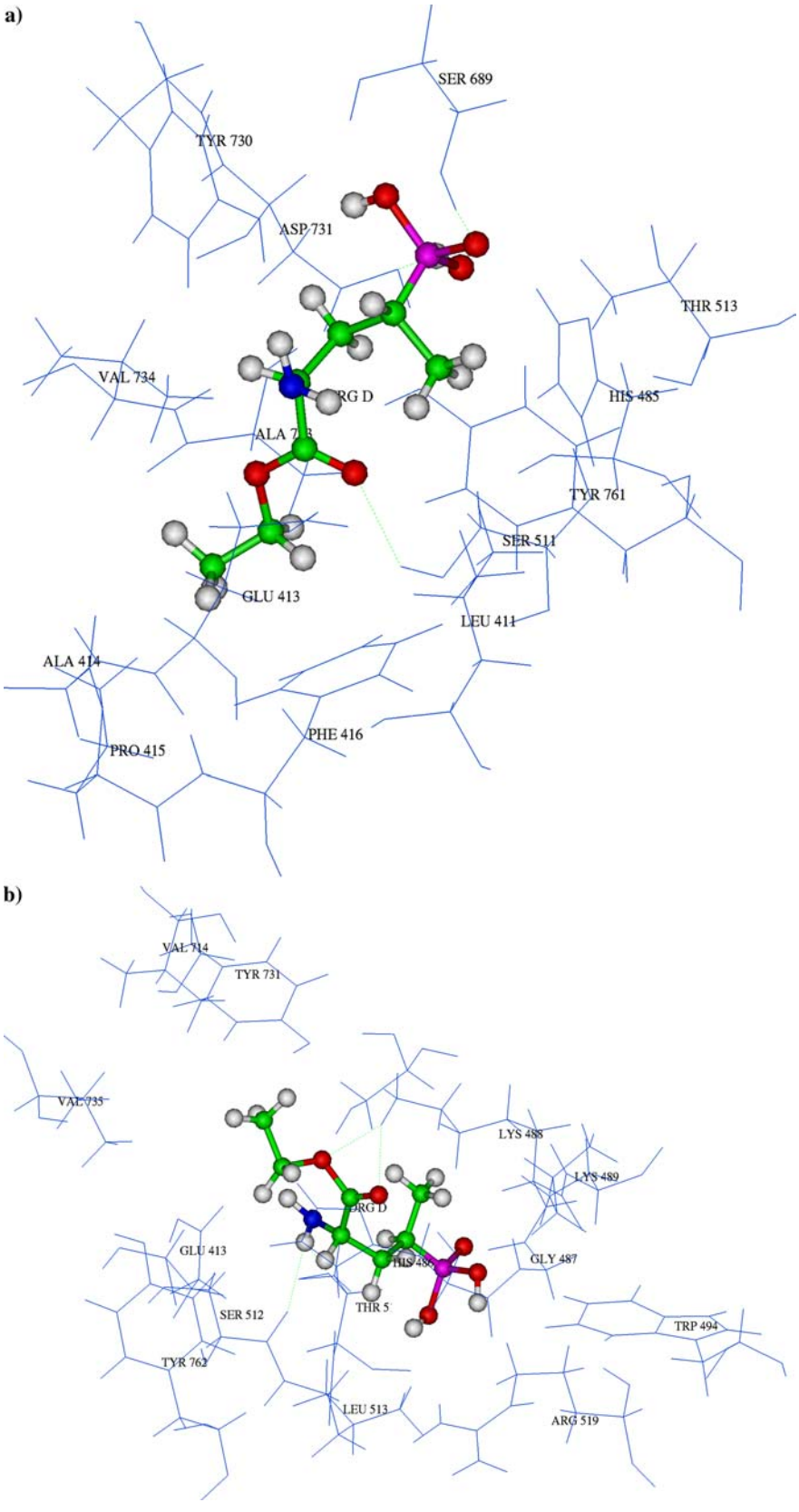


**Fig. 6** **a** shows the interactions of Drug-D with the NR2A subunit of the NMDA receptor. **b** show the interactions of Drug-D with NR2B subunit of the NMDA receptor. The amino acids shown here are within 4 Å radius of drug. Hydrogen bonds between the drug and receptor are marked in *green dotted lines*. Drugs are rendered in cpk (*ball* and *stick*) and amino acids are shown in *blue color* (*lines*)

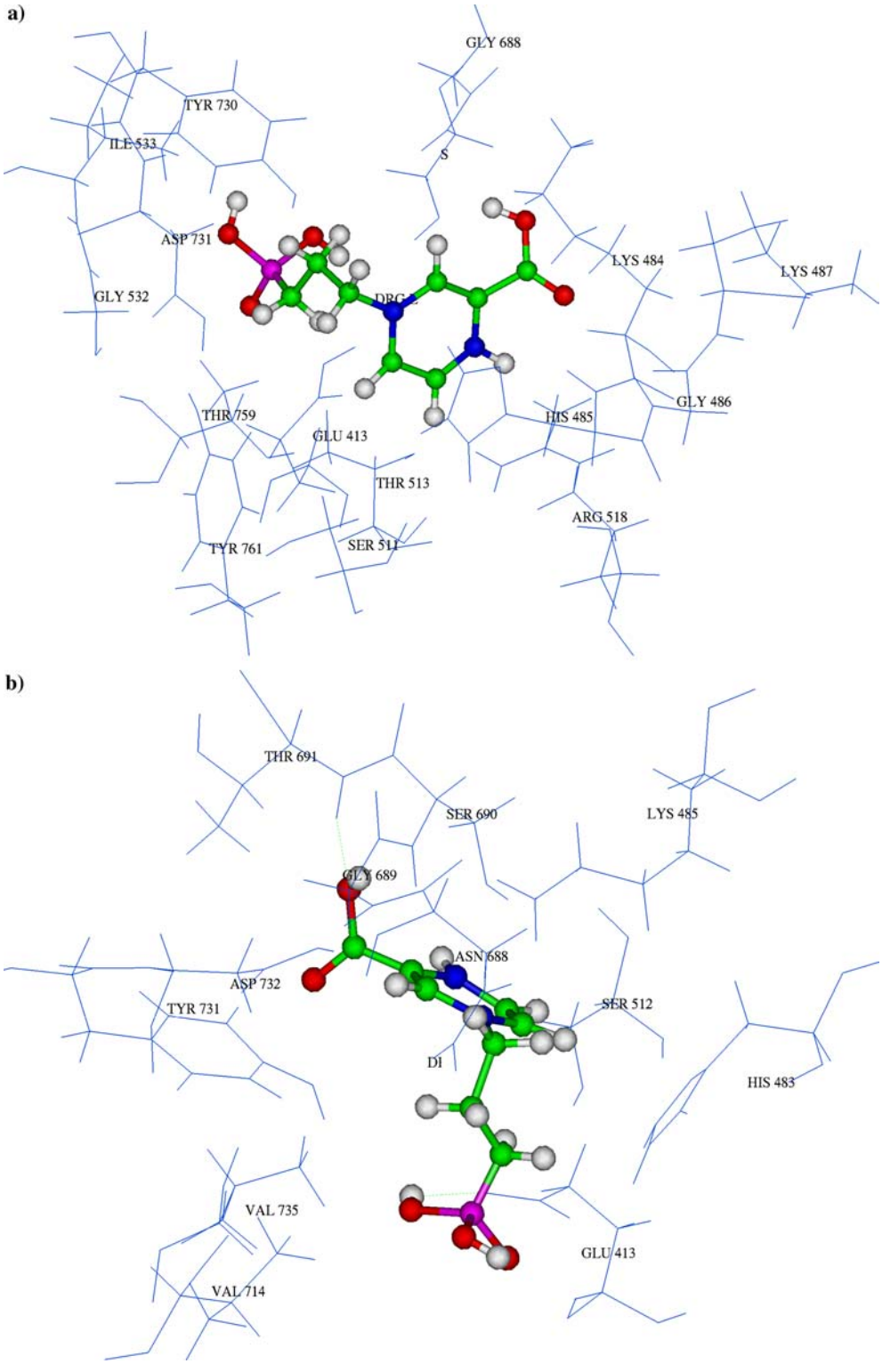


**Fig. 7** **a** shows the interactions of Drug-E with the NR2A subunit of the NMDA receptor. **b** show the interactions of Drug-E with NR2B subunit of the NMDA receptor. The amino acids shown here are within 4 Å radius of drug. Hydrogen bonds between the drug and receptor are marked in *green dotted lines*. Drugs are rendered in cpk (*ball* and *stick*) and amino acids are shown in *blue color* (*lines*)

## Discussion

Sequence analysis and alignment reveal that the NR2A and NR2B subunits of the NMDA receptor are very closely related proteins, having more than 80% sequence identity at their ligand-binding (S1S2) core though divergent for the intracellular C-terminal domain of the intact receptor. Fourteenth and 15th β-strands and the *J-α-helix* of the S2 domain pass through the S1 domain and interact with S1 domain amino acids, forming a clamshell like structure. The S1 domain of the ligand-binding core is formed by ~130 residues located between the amino terminal domain (ATD) and the first transmembrane

**Table 3** Distance between the C-α atoms of six residues forming the ligand-binding pocket in NR2A and NR2B subunits of NMDA receptor

| Distance (Å) | Drug-A | | Drug-B | | Drug-C | | Drug-D | | Drug-E | |
|---|---|---|---|---|---|---|---|---|---|---|
| | NR2A | NR2B | NR2A | NR2B | NR2A | NR2B | NR2A | NR2B | NR2A | NR2B |
| AB | 8.16 | 10.00 | 8.05 | 10.57 | 11.03 | 13.21 | 8.18 | 9.69 | 9.66 | 9.89 |
| BC | 12.35 | 13.77 | 13.09 | 14.22 | **12.84** | **19.31** | 11.12 | 12.72 | 13.41 | 14.50 |
| CD | 7.30 | 9.02 | 7.36 | 8.52 | 8.26 | 7.65 | 5.46 | 7.37 | 7.18 | 7.93 |
| DE | 5.34 | 6.40 | 5.02 | 5.78 | 5.70 | 5.75 | 5.91 | 5.74 | **5.38** | **16.04** |
| EF | 8.77 | 8.49 | 10.33 | 11.06 | 11.07 | 11.76 | 10.83 | 10.86 | **8.85** | **16.55** |
| FA | **9.15** | **15.85** | 9.63 | 8.14 | 8.76 | 10.60 | 11.15 | 9.15 | 10.10 | 10.38 |

In NR2A:A-Ser689; B-Tyr731; C-Glu413; D-Ser511; E-Thr513; F-His485
In NR2B:A-Ser690; B-Tyr731; C-Glu413; D-Ser511; E-THR514; F-LYS484
The difference between the values of NR2A and NR2B is more than 5 Å are in *bold*

**Table 4** Drug–receptor binding score by Ludi scoring methods

| Scoring Paramaters | Drug-A | | Drug-B | | Drug-C | | Drug-D | | Drug-E | |
|---|---|---|---|---|---|---|---|---|---|---|
| | NR2A | NR2B | NR2A | NR2B | NR2A | NR2B | NR2A | NR2B | NR2A | NR2B |
| Hbond[a] | 3 | 2 | 1 | 1 | 1 | 1 | 4 | 5 | 0 | 3 |
| Lipophilic Score[b] | 162 | 106 | 236 | 210 | 153 | 186 | 204 | 206 | 304 | 287 |
| % Contact[c] | 66 | 58 | 60 | 70 | 67 | 76 | 65 | 75 | 74 | 60 |
| Rotational Score[d] | 5–126 | 5–126 | 7–177 | 7–177 | 4–101 | 4–101 | 5–126 | 5–126 | 4–101 | 4–101 |
| Total Binding Score[e] | -38 | -115 | -36 | -60 | -43 | 54 | 251 | 443 | 109 | 170 |

[a] *Hbond* number of hydrogen bonds between drug and receptor
[b] *Lipophilic score* score from the Lipophilic term of scoring function
[c] *Contact* percent of drug-surface in contact with receptor
[d] *Rotational Score* ($\Delta G_{rot}$) represents the contribution by freezing the internal degrees of freedom of a molecule
[e] *Binding score* Ludi scoring function for free energy term

helix (M1). The residues present in the region between M3 and M4 also contribute for a functional S1 domain. Our previous study on the agonist–receptor interaction with the NR2A and NR2B subunits explains the difference in glutamate binding with these two subunits [51]. Compared to the NR2B subunit, NR2A has a higher affinity towards antagonists and lower affinity towards agonists [19, 38–40, 53]). In the present study, competitive antagonists have been docked into the ligand-binding core of NR2A and NR2B subunits. Our docking results show that none of the five drugs have interact similarly with these two different but closely related NMDA receptor subunits. This is inferred by examining the following parameters: (1) residues involved in interaction with the antagonist, (2) classification and description of the interaction sites according their spatial location in the ligand-binding pocket, (3) hydrogen bonding pattern, (4) the difference in the distance between the C-α atoms of the six residues of $c_{\alpha}$-NR2A and 2B subunits involved in ligand binding and (5) the binding-score analysis. Several hydrogen bonds are formed between the electronegative oxygen atoms in the drug molecules are residues in the NR2A and NR2B subunits except the hydrogen bonds between *drug-b* and NR2A, which are formed by the third and fifth hydrogen atom of *AP7* with OG1 of *Thr513* and OD1 of Asp197, respectively. Table 2 shows the patterns of hydrogen bonding between the antagonists and the residues.

Comparatively, all the drugs except *drug-a* and *drug-e* show significant bonded and non bonded interactions, more with the S1 domain residues than with the S2 domain in the NR2B subunit. *Drug-c* shows equal preferences for the S1 and S2 domains in the NR2A subunit. The numbers of interacting residues are different at the interaction sites, while there are similarities in binding pocket residues for *drug-a* and *drug-e* at NR2A and NR2B subunit. The loop region between 6β and 7β, named the second interaction site in Table 1, is crucial in forming charge-dependent—interactions with the receptor as this region is thickly populated with the proton rich *Lys* residues. Moreover, all five drugs are found to interact with this second interaction site of both NR2A and NR2B subunits. On the other hand, the residues located at the third interaction site, i.e. the region between *8*β and *C-α-helix* contribute to hydrophilic interactions with the drug molecules due to the presence of a reactive hydroxyl side chain in residues *Ser* and *Thr* (511 and 513 in NR2A; 512 and 514 in NR2B). In a similar way, the residues present at the *E-α-helix* of the S2 domain provide a hydrophilic pocket due to the presence of the conserved *Ser and Thr* (511 and 513 in NR2A; 512 and 514 in NR2B) residues. *Arg518*/*Arg519* residues (NR2A and NR2B, respectively) determine subunit and drug specific interactions. All the drugs interact with these residues at least in one of the subunits. In other words, these two residues characterize

dug selectivity of the five antagonists studied here. The *Arg* molecule makes a bonded interaction with the ligand, and its absence may influence the drug–receptor interaction, resulting in major dissimilarities among NR2A and NR2B subunits. All the drugs interact with first and sixth interaction sites except for *drug-c* in the NR2B subunit.

The S1S2 domain apo (unbound) state conformation is associated with competitive antagonist effects in ionotropic NMDA receptors. It is conjectured that the wide separation of the S1 and S2 domains results in enhanced antagonist activity [25, 26]. The S1S2 domain remains slightly opened when bound with partial antagonists whereas it is completely detached (like the open-apo conformation) upon binding with full antagonists. Further, during the opening of the S1S2 core, the S2 domain shows considerable higher *rmsd* than the S1 domain [54, 55]. The up and down movement of the S2 domain results in the open and closed conformational transitions while the S1 domain is left less mobile or static. The interactions of *drug-b* and *drug-c* to NR2B may be ascribed to interactions of fewer residues of the S2 domain than for *drug-a* and *drug-e*. In the NR2A subunit, almost all the drugs have similar interactions with the S2 domain except *drug-b*, which has no interaction with the *E-α-helix* of S2 domain. This information visualizes the essential role of the location of interactive residues in the ligand-binding pocket and explains differential effects of various antagonists.

The difference in antagonist activity may be due to the unequal electrostatic potential inside the binding pockets of the NR2A and NR2B subunits of the NMDA receptor, despite ~80% identity with each other and the residues directly interacting with ligand remaining identical in both subunits. This reveals that not only the residues directly interacting with the ligand regulate the binding properties, but the non-conserved amino acids located far from the binding pocket also contribute to ligand binding. The geometry of the ligand-binding pocket in NR2A and NR2B do not show identical architecture. This may produce the difference in electrostatic potential inside the pocket, thereby influencing antagonist affinity and the subunit selectivity. A comparative analysis of LUDI binding scores of the five drugs indicate *drug-d* to bind more effectively with the receptor than other drugs. It also points to *drug-d* and *drug-e* having relatively more interaction with—NR2B than with the NR2A subunit. This information may be useful in the design and development of a subunit-specific antagonist.

## Conclusion

This study provides a microscopic view into the interactions of different NMDA competitive antagonists with the NR2A and NR2B subunits. Seven major interaction sites, including their secondary structure have been identified to be directly involved in receptor-antagonist interactions. We have described two conserved hydrophilic binding pockets: one at S1 (*Ser-Leu-Thr*) and other at the S2 (*Ser-Thr*) domain interface in both NR2 subunits. The *Ser-Leu-Thr* pocket of NR2 is substituted by *Pro-Leu-Thr* in NR1. A *Lys* rich region (second interaction site) equivalent to the loop two region in the NR1 subunit [26] is crucial for antagonist interaction as most of the antagonists interact with this region. The natures of bonded interactions of antagonists are distinct for NR2A and NR2B with *Arg* (Arg518 and Arg519) residue located in the fourth interaction site. The difference in binding-pocket geometry and binding-score lead to the conclusion that the competitive antagonism at NR2A and NR2B subunits of the NMDA receptor is not qualitatively similar. Further studies in this area may aid in the development of subunit-specific NMDA receptor antagonists having lesser side effects than the non-selective compounds.

**Acknowledgment** The authors acknowledge the assistance of Mr. R. Rajagopal in the preparation of the manuscript.

## References

1. McBain CJ, Mayer ML (1994) Physiol Rev 74:723–760
2. Collingridge GL, Bliss TV (1995) Trends Neurosci 18:54–56
3. Choi DW, Koh JY, Peters SJ (1988) J Neurosci 8:185–196
4. Nakanishi S (1992) Science 258:597–603
5. Hollmann M, Maron C, Heinemann S (1994) Neuron 13:1331–1343
6. Rigby M, Le Bourdelles B, Heavens RP, Kelly S, Smith D, Butler A, Hammans R, Hills R, Xuereb JH, Hill RG, Whiting PJ, Sirinathsinghji DJ (1996) Neuroscience 73:429–447
7. Wenzel A, Fritschy JM, Mohler H, Benke D (1997) J Neurochem 68:469–478
8. Monyer H, Burnashev N, Laurie DJ, Sakmann B, Seeburg PH (1994) Neuron 12:529–540
9. Laube B, Kuhse J, Betz H (1998) J Neurosci 18:2954–2961
10. Benveniste M, Mayer ML (1991) Br J Pharmacol 104:207–221
11. Clements JD, Westbrook GL (1991) Neuron 7:605–613
12. Hirai H, Kirsch J, Laube B, Betz H, Kuhse J (1996) Proc Natl Acad Sci USA 93:6031–6036
13. Laube B, Hirai H, Sturgess M, Betz H, Kuhse J (1997) Neuron 18:493–503
14. Anson LC, Chen PE, Wyllie DJ, Colquhoun D, Schoepfer R (1998) J Neurosci 18:581–589
15. Hawkins LM, Chazot PL, Stephenson FA (1999) J Biol Chem 274:272–118
16. Chazot PL (2000) Curr Opin Investig Drugs 1:370–374
17. Chenard BL, Menniti FS (1999) Curr Pharm Des 5:381–404
18. Priestley T, Laughton P, Macaulay AJ, Hill RG, Kemp JA (1996) Neuropharmacology 35:1573–1581
19. Priestley T, Laughton P, Myers J, Le Bourdelles B, Kerby J, Whiting PJ (1995) Mol Pharmacol 48:841–848
20. Buller AL, Monaghan DT (1997) Eur J Pharmacol 320:87–94
21. Feng B, Tse HW, Skifter DA, Morley R, Jane DE, Monaghan DT (2004) Br J Pharmacol 141:508–516
22. Monaghan DT, Olverman HJ, Nguyen L, Watkins JC, Cotman CW (1988) Proc Natl Acad Sci USA 85:9836–9840
23. Ortwine DF, Malone TC, Bigge CF, Drummond JT, Humblet C, Johnson G, Pinter GW (1992) J Med Chem 35:1345–1370
24. Stern-Bach Y, Bettler B, Hartley M, Sheppard PO, O'Hara PJ, Heinemann SF (1994) Neuron 13:1345–1357
25. Armstrong N, Gouaux E (2000) Neuron 28:165–181
26. Furukawa H, Gouaux E (2003 ) EMBO J 22:2873–2885

27. Oh BH, Pandit J, Kang CH, Nikaido K, Gokcen S, Ames GF, Kim SH (1993) J Biol Chem 268:11348–11355
28. Jin R, Banke TG, Mayer ML, Traynelis SF, Gouaux E (2003) Nat Neurosci 6:803–810
29. Chohan KK, Wo ZG, Oswald RE (2000) J Mol Mod 6:16–25
30. Tikhonova IG, Baskin II, Palyulin VA, Zefirov NS, Bachurin SO (2002) J Med Chem 45:3836–3843
31. Foucaud B, Laube B, Schemm R, Kreimeyer A, Goeldner M, Betz H (2003) J Biol Chem 278:24011–24017
32. Laube B, Schemm R, Betz H (2004) Neuropharmacology 47:994–1007
33. Sanchez R, Sali A (1997) Curr Opin Struct Biol 2:206–214
34. Bi H, Sze CI (2002) J Neurol Sci 200:11–18
35. Leeson PD, Carling RW, Moore KW, Moseley AM, Smith JD, Stevenson G, Chan T, Baker R, Foster AC, Grimwood S (1992) J Med Chem 35:1954–1968
36. Woodward RM, Huettner JE, Guastella J, Keana JF, Weber E (1995) Mol Pharmacol 47:568–581
37. Christie JM, Jane DE, Monaghan DT (2000) J Pharmacol Exp Ther 292:1169–1174
38. Buller AL, Larson HC, Schneider BE, Beaton JA, Morrisett RA, Monaghan DT (1994) J Neurosci 14:5471–5484
39. Grimwood S, Gilbert E, Ragan CI, Hutson PH (1996) J Neurochem 66:2589–2595
40. Kendrick SJ, Lynch DR, Pritchett DB (1996) J Neurochem 67:608–616
41. Altschul SF, Madden TL, Schaffer AA, Zhang J, Zhang Z, Miller W, Lipman DJ (1997) Nucleic Acids Res 25:3389–3402
42. Rost B, Sander C, Rost B, Sander C (1993) J Mol Biol 232:584–599
43. Thompson JD, Higgins DG, Gibson TJ (1994) Nucleic Acids Res 22:4673–4680
44. Sali A, Blundell TL (1993) J Mol Biol 234:779–815
45. Luthy R, Bowie JU, Eisenberg D (1992) Nature 356:83–85
46. Laskowski RA, MacArthur MW, Moss DS, Thornton JM (1993) J Appl Crystal 26:283–291
47. All tools utilized herein were accessed and utilized as implemented in InsightII-97.5, Accelrys (www.accelrys.com)
48. Kleywegt GJ, Jones TA (1997) Methods in Enzymology 277:525–545
49. Bohm HJ (1992) J Comput Aided Mol Des 6:593–606
50. Bohm HJ (1994) J Comput Aided Mol Des 3:243–256
51. Blaise M, Sowdhamini R, Rao MRP, Pradhan N (2004) J Mol Model (in press)
52. Evans RH, Francis AA, Jones AW, Smith DA, Watkins JC (1982) Br J Pharmacol 75:65–75
53. Laurie DJ, Seeburg PH (1994) Eur J Pharmacol 268:335–345
54. Pang A, Arinaminpathy Y, Sansom MS, Biggin PC (2003) FEBS Lett 550:168–174
55. Arinaminpathy Y, Sansom MS, Biggin PC (2002) Biophys J 82:676–683